Modelling of Advection-Dominated Transport in a Porous Column with a Time-Decaying Flow Field

A. P. S. SELVADURAI⋆ and W. DONG
Department of Civil Engineering and Applied Mechanics, McGill University, 817 Sherbrooke Street West, Montreal, QC, Canada H3A 2K6

Abstract. This paper examines the problem of the advective-dispersive movement of a non-decaying, inert chemical dye solution through the pore space of a fluid saturated porous column. The objective of the paper is to present a complete study of the one-dimensional advective-dispersive transport problem by considering certain analytical solutions, experimental results and their comparisons with specific computational simulations. Dye concentrations obtained by means of an image processing method are used in conjunction with an analytical solution to identify the hydrodynamic dispersion coefficient that governs the advective-dispersive transport problem. The experimental results and identified parameters are also used to assess the computational estimates derived from several stabilized computational schemes available in the literature, for examining advection-dominated transport processes in porous media.

Key words: advective-dispersive transport, transport in a column, parameter identification, image analysis, computational modelling, experimental modelling.

1. Introduction

The study of contaminant migration in porous geologic media is a topic of current importance to environmental applications involving earthborne movement of hazardous wastes, pollutants and other chemicals (Bear, 1972; Philips, 1991; Bear and Bachmat, 1992; Banks, 1994). In geologic media, groundwater constitutes the main agency for the transportation of such contaminants. The physico-chemical processes contributing to the transport of contaminants are generally quite complex and determined by the physical and geochemical properties of both the porous geologic medium and the chemical species that is being transported. In relation to modelling

---

⋆Author for correspondence: e-mail: patrick.selvadurai@mcgill.ca

transport problems in porous media, it is generally assumed that transport can take place both through advection, due to the movement of chemicals with fluid flow, and an effective dispersion process that can include both molecular diffusion due to concentration gradients and mechanical dispersion due to momentum transfer. (Mathematically both processes can be described by a similar governing equation.) The classical advection-dispersion equation represents a highly simplified model of a complex set of transport processes, which can also be influenced by a variety of nonlinear phenomena, including chemical absorption and chemically-induced alterations of fluid transport characteristics of the porous medium. Despite these limitations, the classical advection-dispersion equation is widely used to examine contaminant transport in porous media. The justification for this simplified approach is readily provided by the ease with which the simplified models can be used to examine variability in the physical parameters governing the advective-dispersive transport process. The mathematical similarities also extend the application of the equation to other geophysical problems including, creeping movement of glaciers, sediment and salt movement in the oceans and geothermal energy extraction. The study of the classical advection-dispersion-type equations through analytical means can be attempted only in a limited number of cases involving either a single spatial dimension or a high degree of spatial symmetry. Selvadurai (2002, 2003, 2004a, b) has recently developed exact closed-form analytical solutions to three-dimensional problems involving advective flows. For other realistic practical situations involving advective-dispersive transport, recourse must be made to computational procedures. The progress made over the past three decades in the computational approaches to the study of the advection-dispersion equations is quite considerable and no attempt will be made to provide a comprehensive review of this area. Certain key contributions in this area include the works of Raymond and Garder (1976), Hughes and Brooks (1982), Vichnevetsky and Bowles (1982), Donea et al. (1984), Morton (1996) and Oñate et al. (1997). Examples that evaluate the computational performance of schemes used to model both advective and advective-dispersive flows in single and double porosity media are given by Zhao and Valliappan (1994), Valliappan et al. (1998), Wendland and Schmid (2000) and Wang and Hutter (2001).

This paper examines the problem of one-dimensional advective-dispersive transport of a chemical in a porous medium from three inter-related aspects: analytical, computational and experimental. The mathematical treatment of the classical one-dimensional equation of the advective-dispersive type has a long history commencing with the work of Light-foot (1929) dealing with the cooling of molten steel. Despite its simplicity, relatively few attempts have been made to experimentally verify the

accuracy of the mathematically modelling. Taylor (1953) was perhaps the first to apply the advection-dispersion equation to examine the dispersion of soluble matter in a solvent due to flow in a tube. Ogata and Banks (1961) developed an analytical solution to the one-dimensional partial differential equation governing the advective-dispersive transport problem. Lindstrom *et al.* (1967) and Banks (1994) applied the classical advective-diffusive transport theory to the study of geo-environmental problems including herbicide movement in soil and give further references to pertinent literature. These and other studies related to the classical one-dimensional advection-dispersion equation deal with problems where the advective flow velocity is constant. Problems dealing with variable velocity fields have been discussed in connection with the stochastic equations applicable to the advective-dispersive transport problem (Gelhar, 1993). More recently, Shvidler and Karasaki (2003a, b) and Dagan (2004) have examined the one-dimensional transport problem where the flow velocity is stochastic. If Darcy flow exists in a homogeneous porous medium that is non-deformable and the permeating fluid is incompressible, then for the flow to be time-dependent the boundary potential should vary with time and the domain must be finite. If either the pore fluid or the porous medium is deformable, then there are no restrictions on the spatial extent of the one-dimensional domain and the flow velocities can be both time- and space-dependent. In this paper, we restrict attention to the study of the one-dimensional advection-dispersion transport problem where the velocity varies exponentially with time due to an exponential variation in the boundary potential. The problem arises in a simple one-dimensional experiment, which involves gravity-induced falling head at one boundary of the porous domain (Figure 1). Analytical solutions to initial boundary value problems involving the advection-dispersion equation, for the case where the velocity varies exponentially with time, are not available in the literature. This makes both the analysis of experimental data and the validation of computational methods developed for examining the advection-dispersion equation difficult exercises. The primary objective of the research is to examine the problem of advective-dispersive transport in the fluid-saturated porous column particularly in the presence of time-dependent flow velocities and to assess the predictive capabilities of the computational approaches to the modelling of the advection-dominated transport with time-dependent advective velocity fields. To aid this exercise, recourse is also made to the study of the classical one-dimensional advective-dispersive transport problem that serves in a parameter identification exercise for determining the dispersivity characteristics governing the transport process.

Figure 1. The porous column test facility.

2. The Advection-Dispersion Equation

We consider the problem of the one-dimensional non-reactive advective-dispersive transport of a chemical species in a fluid saturated porous medium, for which Darcy flow is applicable and the governing partial differential equation is given in the references cited previously. For one-dimensional conditions and under a flow velocity that is independent of the spatial variable but has a time-dependency with an exponential form, the partial differential equation governing advective-dispersive transport takes the form

$$\frac{\partial C}{\partial t} + v_0 \exp\left(-\lambda t\right)\frac{\partial C}{\partial x} = D\frac{\partial^2 C}{\partial x^2}, \tag{1}$$

where $C(x, t)$ is the concentration of the chemical measured per unit volume of the fluid, x is a spatial coordinate, t is time and D is the hydrodynamic dispersion coefficient, the composition of which will be discussed later. The parameter λ occurring in (1) can be interpreted by appeal to Darcy flow in a one-dimensional column of length l, and in this case $\lambda = k/l$. Since the fluid velocity is defined in relation to the pore space, k is the Dupuit–Forchheimer measure of hydraulic conductivity of the porous medium, which is related to the conventional Darcy value applicable to the area averaged hydraulic conductivity $\tilde{k}$, through the relationship $k = \tilde{k}/n^*$, and n^* is the porosity of the porous medium. Also, we denote the velocity $v_0 = k(H_0 - H_D)/l$, where H_0 and H_D can be identified as the inlet and outlet potentials at the start of the advective flow process. The chemical is also assumed to occupy a part of the column at the start of the advective flow process. To the authors' knowledge there are no closed form solutions to initial boundary value problems associated with finite regions. An assumption that is generally invoked in relation to the development of solutions of (1) with $\lambda = 0$ (i.e. constant advective velocity) is to consider the one-dimensional region to be of finite extent with regard to the development of advective flow but consider the same region to be either infinite or semi-infinite with respect to the development of advective-dispersive and/or advective-diffusive processes. Even with this latter assumption, there appears to be no generalized exact solution available to the initial boundary value problem, governed by the partial differential Equation (1), subject to the initial and boundary conditions

$$C(x, 0) = 0, \quad 0 \leqslant x < \infty, \tag{2}$$
$$C(0, t) = C_0 \mathsf{H}(t), \quad t \geqslant 0, \tag{3}$$

where C_0 is a constant and $\mathsf{H}(t)$ is the Heaviside step function. A simplified solution is always desirable in view of its potential applicability of such a solution in any parameter identification exercise. In view of this observation, we seek solutions to an *initial value problem* of the advective-dispersive transport resulting from the situation where the chemical occupies part of the porous region. The initial condition applicable to the chemically dosed region occupying the idealized infinite domain of the finite or infinite interval $[a, b]$ is taken as

$$C(x, 0) = C_0[\mathsf{H}(x - a) - \mathsf{H}(x - b)], \quad x \in (-\infty, \infty), \tag{4}$$

where $a \leqslant b$. A solution to the initial value problem of the advective-dispersive transport of a chemical plug of finite extent moving in a porous column, which is considered to be of finite extent with respective to the advective flow but of infinite extent with respect to the advective-diffusive transport, was first presented by Selvadurai (2004b). Generalizing this

result, the resulting solution to the initial value problem defined by the partial differential Equation (1) and the initial condition (4) can be expressed in the form

$$\frac{C(x,t)}{C_0} = \frac{1}{2}\mathrm{erf}\left(\frac{-x - a + v_0\frac{\{1-\exp(-\lambda t)\}}{\lambda}}{2\sqrt{Dt}}\right) -$$

$$-\frac{1}{2}\mathrm{erf}\left(\frac{-x - b + v_0\frac{\{1-\exp(-\lambda t)\}}{\lambda}}{2\sqrt{Dt}}\right), \quad x < v_0t, \tag{5a}$$

$$\frac{C(x,t)}{C_0} = \frac{1}{2}\mathrm{erfc}\left(\frac{x - b - v_0\frac{\{1-\exp(-\lambda t)\}}{\lambda}}{2\sqrt{Dt}}\right) -$$

$$-\frac{1}{2}\mathrm{erfc}\left(\frac{x - a - v_0\frac{\{1-\exp(-\lambda t)\}}{\lambda}}{2\sqrt{Dt}}\right), \quad x \geqslant v_0t, \tag{5b}$$

where $\mathrm{erfc}(\alpha)$ is the complimentary error function defined in terms of the error function $\mathrm{erf}(\alpha)$ through the relation

$$\mathrm{erf}(\alpha) = 1 - \mathrm{erfc}(\alpha) = \frac{2}{\sqrt{\pi}}\int_0^\alpha \exp(-\varsigma^2)\,\mathrm{d}\varsigma. \tag{6}$$

The purpose of developing analytical solutions to either the *initial value problem* defined by (1) and (4) or the *initial boundary value problem* defined by (1)–(3) largely relates to their importance in connection with the validation of experimental modelling and computational schemes developed for the treatment of the advection-dispersion equation. Almost every validation exercise involving computational treatments and the analytical solution of the one-dimensional advective-dispersive transport problem assumes that the advective velocity is constant throughout the domain. The solution for the initial boundary value problem with a constant flow velocity, applicable to a semi-infinite domain and defined by the initial and boundary conditions (2) and (3), respectively, was given by Ogata and Banks (1961) as follows:

$$\frac{C(x,t)}{C_0} = \frac{1}{2}\left[\mathrm{erfc}\left(\frac{x - v_0t}{2\sqrt{Dt}}\right) + \exp\left(\frac{xv_0}{D}\right)\mathrm{erfc}\left(\frac{x + v_0t}{2\sqrt{Dt}}\right)\right]. \tag{7}$$

3. The Advective-Dispersive Flow Experiment and Image Analysis

3.1. ADVECTIVE-DISPERSIVE TRANSPORT IN A POROUS COLUMN

The configuration of the one-dimensional column used in the experiment is shown in Figure 1. The apparatus consists of a series of precision manufactured glass cylinders of diameter 15 cm, length 61 cm and wall thickness 0.50 cm, which are connected to form the one-dimensional column of
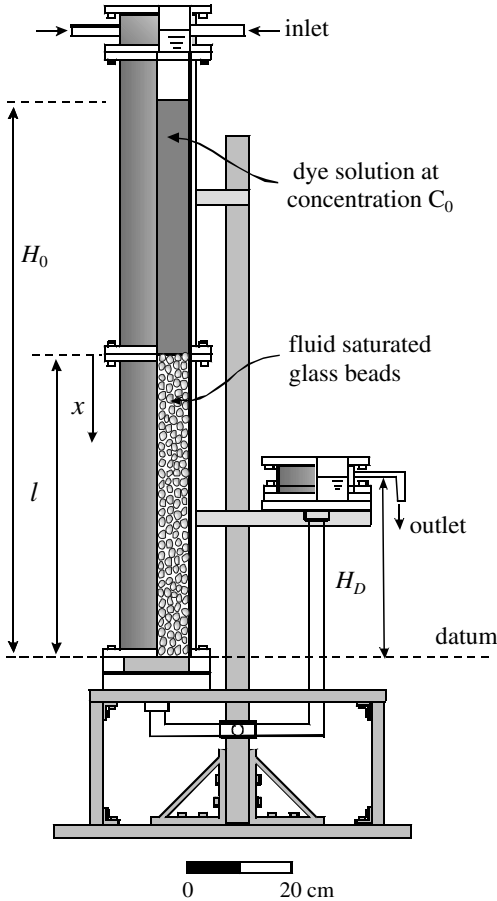
Figure 2. A schematic view of the porous column experiment for examining advective diffusive transport processes in a fluid-saturated porous column.

length 102 cm (Figure 2). The choice of the smooth-walled glass cylinders is both to minimize damage due to scratching of the interior surface by the glass beads used for the porous material and to provide a relatively distortion-free transparent surface through which the migration of the chemical dye within the porous medium can be observed. The porous medium used in the experiments consists of a mixture of spherical Ballotini glass beads with specific gravity of approximately 2.5 and diameter varying between $150\,\mu$m and $212\,\mu$m. This granular material is placed in the column of water of height 61 cm to a porosity corresponding roughly to 38.5%. For glass spheres, the theoretical estimates for the porosity range from 47.5% for a cubic packing to 26% for a rhombohedral packing. The hydraulic conductivity of the porous medium is calculated using results of both constant and variable head tests, and it is estimated to be approximately

$\tilde{k} = 2.0 \times 10^{-4}$ m/s. A water soluble *sodium chloride acid red dye* is used in the experiments. The chemical dye solution mixed in the proportion of 1 g/L of pure water occupies the region above the saturated glass bead column. Careful placement of the chemical dye solution is necessary to eliminate the premature migration of the chemical dye into the porous region and, essentially, the section of the column with the porous medium can be regarded as being free of any chemical dye. Furthermore, since the preparation time for the experiment is relatively small (less than 30 mins) the diffusion from the column of dye solution to the saturated porous column can be neglected.

The test facility was used to conduct the advective-dispersive transport experiments where a non-reactive, non-decaying chemical dye solution was allowed to move through the fluid-saturated porous column with either a constant flow velocity or a time-dependent flow velocity. In the *constant flow velocity transport experiment*, the chemical dye solution is allowed to migrate through the porous medium under a constant hydraulic potential gradient that maintains a steady advective flow velocity over the length of the porous medium. This constant potential gradient is initiated by maintaining inlet and outlet hydraulic potentials constant at the upper and lower ends of the porous column, respectively. In the experiment involving transport with a *time-dependent flow velocity*, a section of the test column containing the chemical dye solution is filled with glass beads to approximately the same porosity as the porous material in the water-saturated region, and chemical dye solution is allowed to migrate through the porous column under a decaying hydraulic head at inlet boundary of the porous column, which gives rise to a spatially constant advective flow velocity but with an exponential variation in time. Using the time-dependent flow velocity configuration, the *transport of a plug of the chemical dye* within the porous column is also examined. The column consists of three sequential layers of glass beads, with each separate region saturated with water, with the chemical dye solution and again saturated with water. During the preparation of the three-region porous column, the glass beads are first placed in the column of water until the level of the porous column reaches a height that would correspond to one boundary of the chemical plug. The excess water above the glass beads is then drained until the water level reaches the surface of the column of saturated glass beads. The chemical dye solution at a fixed concentration is now carefully added to the glass container avoiding disturbance of the interface. Additional glass beads are gently placed into the dye solution until the required height of chemical plug is achieved. The excess chemical dye solution above this plug is removed by suction. Saturated glass beads are now placed to isolate the chemical plug and water is added to fill the column. Further glass beads are now added to the column to the required height. The column is now

Table I. The initial inlet and outlet potential heads for different transport processes in porous column

	With constant flow	With decaying flow	Dye plug
H_0 (m)	0.70	1.02	0.96
H_D (m)	0.45	0.0	0.26

filled with water to ensure that sufficient head is available to initiate a time-dependent advective flow velocity that will result in the movement of the chemical plug. The initial inlet hydraulic potential, H_0 and outlet hydraulic potential H_D applied respectively at the top and base of the column of glass spheres for the three porous column experiments described earlier are listed in Table I.

The movement of the chemical dye solution in the saturated porous column is recorded at certain time intervals by a digital camera with a digital sensor of 5 Mega Pixels. The camera is located in front of the glass tube and at the mid-point level of the region of experimental interest. Since a good contrast of the digital images will generate better data for purposes of image analysis, glass beads of uniform translucent color is used as a porous medium; this provides a suitable contrast to the red color of the chemical dye solution. Strong diffusive light is applied to the entire sample to provide a uniform view and exposure. These features are important for estimating the digitized distribution of the dye concentration by means of color contrast techniques. The images captured by the digital camera contain the two dimensional transport pattern of the chemical dye solution adjacent to the wall of the glass tube. An image strip measuring 1835×40 pixels, selected along the central part of glass bead column, is extracted from the photograph for purposes of image analysis. The details of the image analysis procedure will be discussed in the ensuing section. Since the diameter of the glass tube (15 cm) is much greater than the width of the image strip (less than 0.5 cm), and since the axis of the recording camera is normal to the plane of the image strip, the influence of light distortion due to the thickness of the glass tube can be neglected in the strip under investigation. A typical record of the migration of the chemical dye solution through the porous column for each type of the transport process is shown in Figure 3.

3.2. IMAGE PROCESSING

One key aspect of the experimentation involves the measurement of the concentration of the chemical dye solution in the porous medium during its advective-dispersive transport. An essential constraint on the
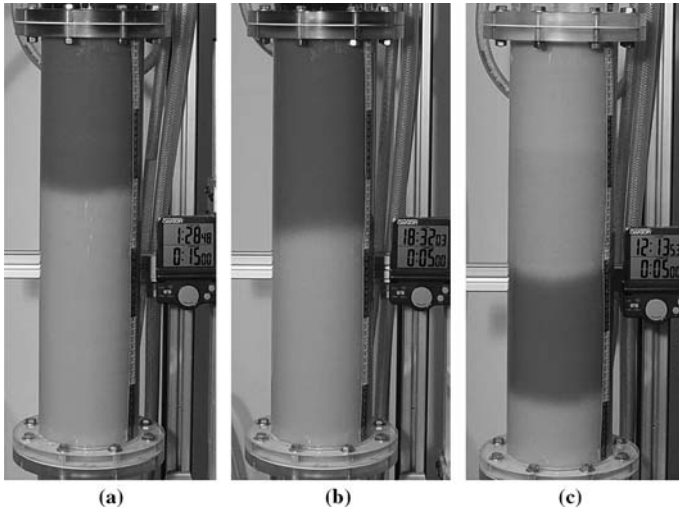
Figure 3. Typical photographic records of transport phenomena in the porous column for three types of transport processes (a) with constant hydraulic potential, (b) with exponentially decreasing hydraulic potential, and (c) movement of a plug of chemical dye.

measurement of the concentration is that the procedure should be non-invasive. The presence of a measuring device within the porous column would represent an anomaly that would influence the flow pattern within the porous medium, which in turn will affect the advective-dispersive transport process. With the advent of efficient technologies for visualization and processing of digital information, digital image processing techniques have been successfully used in a number of areas in the pure and applied sciences and in the environmental sciences. These range from micro-inspection of materials including mapping of defects, medical diagnosis, measurement of travel time of sound waves, monitoring pollutant migration in the oceans by satellite imaging and by remote sensing, weather prediction, mapping of the earth's surface and resources exploration (Gonzalesz and Woods, 2002). Image processing techniques used in medical, chemical, agricultural and geological fields are now regarded as universal tools for visualizing, digitizing and quantifying results of experimental research. In the context of geosciences, digital imaging techniques have also been applied to investigate the structure of porous media and for the examination of the evolution of heterogeneities in porous media due to damage resulting from miscible and immiscible flows (Dawe *et al.*, 1992; Caruana and Dawe, 1996; Garboczi *et al.*, 1999). Such techniques have also been used to examine non-linear phenomena associated with reaction-diffusion processes in the matrices of structured polymers, for the measurement of deformations of geomaterials tested under

triaxial and centrifuge stress states and to examine migration of contaminating oils in unsaturated soils.(Allersma, 1982,1990,1998; Rambidi and Maximychev, 1994; Rambidi *et al.*, 1995; Macari *et al.*, 1997; Esposito et al., 1999; Asundi, 2002). In the current experimental research, the image processing techniques will be used to determine the advective-dispersive transport processes of chemical dye solution within the porous column of glass beads.

Prior to conducting measurements of concentration of the chemical dye solution during its passage through the saturated porous medium, it was necessary to calibrate the concentration level of the chemical dye solution in its *in situ* condition within the porous granular medium. The rationale for this procedure is dictated by the fact that the interpretation of the absolute values of the dye concentration is not assured without recourse to a known reference estimate, since any optical distortions due to reflections from both the glass container and the glass beads can influence the interpretation of the dye concentrations. As a part of the preliminary experimentation, the glass beads were placed to the reference porosity in seven solutions containing known concentrations of the chemical dye, ranging from 0, 0.05, 0.1, 0.25, 0.5, 0.75 to 1.0 g/L of the pore fluid, as shown in Figure 4(a)–(g), to develop a relationship between the *experimentally determined concentrations* of the dye solution associated with pre-defined concentrations and their *colour counterpart within the glass beads* through a colour imaging technique. It is shown from the images of these chemically dosed glass bead columns (Figure 4(h)) that these colour images do vary with the concentration of the chemical dye in the porous medium, and therefore they could serve as the reference basis for interpreting the concentration of the chemical dye solution during its advective-dispersive transport through the porous column.
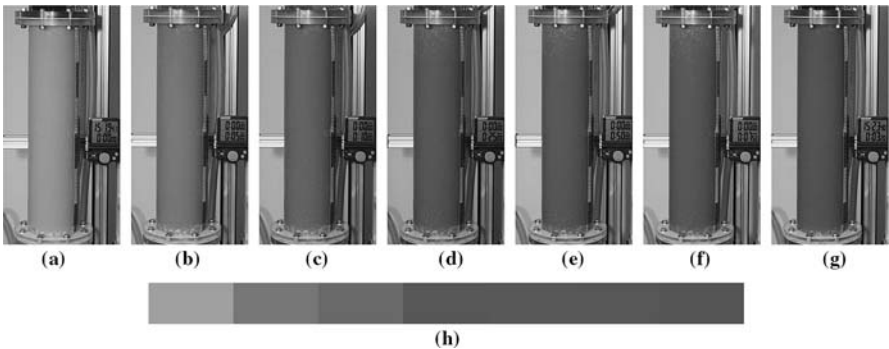

Figure 4. Seven samples used in the calibration exercise with concentration of: (a) 0.0, (b) 0.05, (c) 0.10, (d) 0.25, (e) 0.50, (f) 0.75, (g) 1.00 g/L, and their true-color images (h).

In order to achieve such a correlation it is necessary to perform an analysis of these colour images, which are referred to as *truecolour* images and composed of three components of the primary colours, *r*ed, *g*reen and *b*lue, at each pixel. This decomposition is necessary since the *truecolour* images contain not only the colour distribution of the dye solution within the pore space but also the colour of glass beads in the porous column. In order to obtain the image of the colour of the dye solution within the pore space, the colour of glass beads should be interpreted as noise imposed on the red colour of dye solution, and should be filtered out from the original image. The Figure 5(a) shows the schematic arrangement of a set of 5×5 pixels of a truecolor image. Considering a void ratio $e = 0.64$, approximately 38% of the image of sample is taken up by the dye solution in pore space and the glass beads account for 62% of the image. Therefore on average, 10 of the 25 pixels account for the colour of the dye solution and an average the remaining 15 pixels account for the colour of glass beads. These 25 pixels can be ordered by means of the colour component to make a sorted set (Figure 5(b)). The element within the first 15 ranks in the sorted set, which corresponds to the colour of dye solution in pore space in the 5×5 pixels image, is then chosen and used to replace each pixel in the 5×5 pixels image corresponding to the colour of the glass beads. Finally the colour of the glass beads in the image can be filtered out from the image of the sample (Figure 5(c)).

This filtering technique can be used to examine the seven samples with known concentrations (Figure 4(a)–(g)). These samples represent seven points in the graph of concentration of the dye solution vs. the primary colour components *r*ed, *g*reen and *b*lue taken separately (Figure 6). A *cubic spline interpolation* can be applied to these sample points to generate smooth piecewise polynomial curves for each colour component (Figure 6). These curves reflect the relationship between the concentration of dye solution and its colour counterpart in the pore space of the medium, i.e.
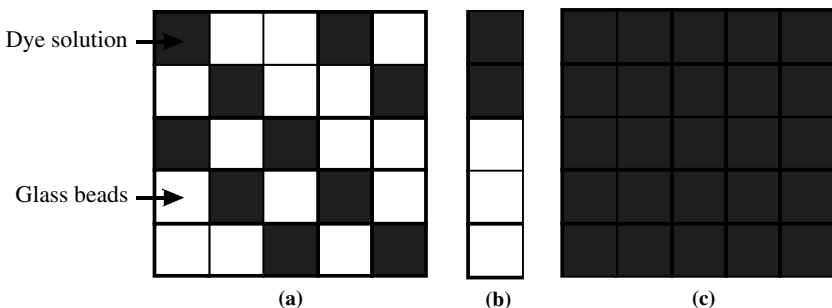

Figure 5. Schematic draft of 5×5 pixels, (a) initial distribution of colour, (b) ranking of colour, (c) redistribution of colour over 5×5 pixels.
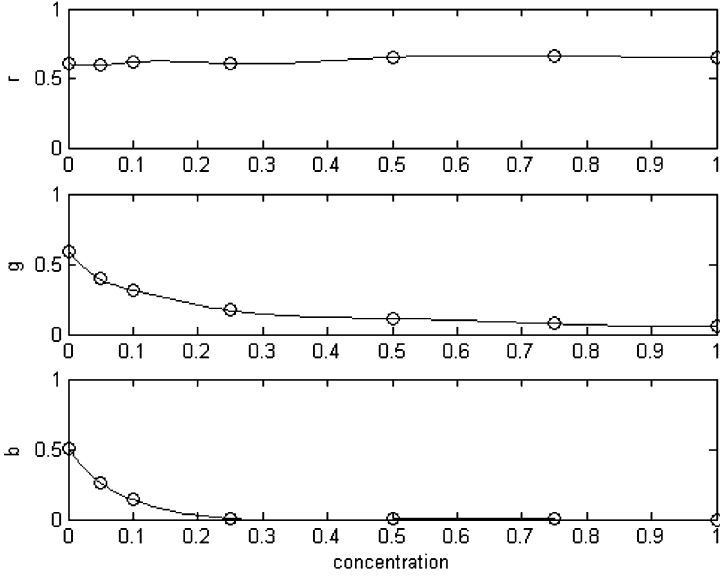
Figure 6. Spline fitted curves of the three primary colour components of the seven samples used in the colour calibration exercise.

$C = C(r, g, b)$, where C is the concentration, $(r, g, b) \in G$ is the colour coordinate associated with C, and G is the range of colour components (r, g, b) determined by the seven samples. These calibration curves can be used to create the *colour map*, which can then be used as the criterion to transform the colour distribution to a quantitative estimate of the dye concentration in the pore space by means of a least squares criterion. We note from Figure 6 that values of the red and blue colour components of the samples with the concentration of 0.5 g/L, 0.75 g/L and 1.0 g/L are almost close to each other and only their green colour component value changes within a small range. This implies that the colour is more sensitive for high concentrations of dye solution in pore space than for low concentrations, and therefore the ambient lighting conditions and digital camera setting during the recording of the transport process in the porous column should be maintained in the same state as that used in the calibration exercises.

Depending upon the type of the column test, a dye solution with a concentration of 1.0 g/L is placed either above or within the porous column. The transport process can be conducted in the column with either a constant or an exponentially decreasing boundary potential, and the progress of the chemical dye solution within the porous column is recorded using the high-resolution digital camera. The images of colour distribution $(r_i^{ob}, g_i^{ob}, b_i^{ob})$ for the dye solution along the porous column can be obtained at specified time intervals. The projected point (r', g', b') of $(r_i^{ob}, g_i^{ob}, b_i^{ob})$ in colour set G created by the samples can be determined by a least squares criterion

$$\big((r_i^{ob} - r')^2 + (g_i^{ob} - g')^2 + (b_i^{ob} - b')^2\big)$$
$$= \min_{(r,g,b) \in G} \big((r_i^{ob} - r)^2 + (g_i^{ob} - g)^2 + (b_i^{ob} - b)^2\big). \tag{8}$$

Substituting (r', g', b') into the colour map $C(r, g, b)$ created via spline fitting curves shown in Figure 6, we can obtain an estimate of concentration of the chemical dye solution at the pixel i

$$C_i = C(r', g', b'). \tag{9}$$

The least-squares criterion (8) implies that *if* the observed colour $(r_i^{ob}, g_i^{ob}, b_i^{ob})$ at the pixel i does not belong to the colour set G, i.e. $(r_i^{ob}, g_i^{ob}, b_i^{ob}) \notin G$, then the projected points (r', g', b') of $(r_i^{ob}, g_i^{ob}, b_i^{ob})$ in G, in terms of the shortest distance, will be used to determine the quantitative value of the concentration of dye solution. Figure 7 shows the results of the digitization procedure, which has been applied to extract the quantitative distribution of the concentration of the dye solution from its colour distribution in the porous medium at a particular time. Figure 8 shows the experimental results for the variation of normalized concentration distribution, C/C_0, in the porous column with a constant hydraulic potential difference as a function of the dimensionless variables $X (= x/l)$ vs. $T (= kt/l)$. These results will be used to determine hydrodynamic dispersion coefficient D or longitudinal dispersivity α_L using an analytical solution and a parameter identification algorithm described in the ensuing section.

4. Identification of the Dispersion Coefficient

4.1. INVERSE ANALYSIS

For a porous medium that is hydraulically homogeneous, the parameters governing the advective-dispersive transport process in the porous column
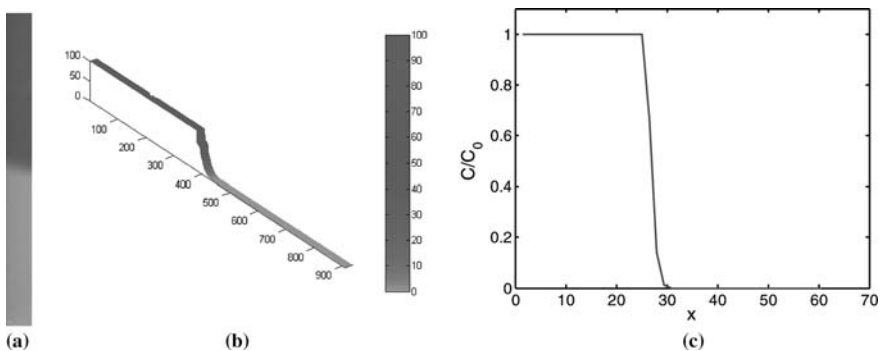

Figure 7. Digitization of the concentration distribution in tube, (a) the image, (b) the transformation from colour to digital image, (c) quantitative distribution of concentration.
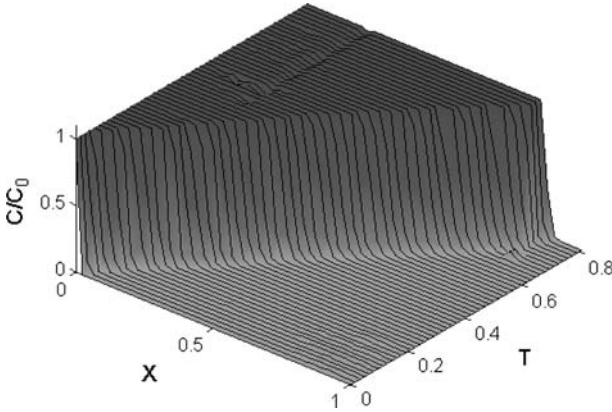
Figure 8. Experimental results for the chemical dye concentration in the porous column with constant flow velocity.

are the advective velocity v_0 and hydrodynamic dispersion coefficient D. The advective velocity both for constant and time-dependent processes can be determined from the knowledge of the hydraulic conductivity of the porous region and its geometry. Therefore, the objective of an inverse analysis is to use the experimental results of distributions of the chemical dye concentration measured along the porous column to determine the dispersion coefficient D applicable to the transport process. This parameter can be identified by solving the optimization problem with an objective function $J(D)$, which is created by using an Output Least Squares (OLS) criterion relating the observed and calculated distributions of the chemical dye concentration: i.e.

$$
\begin{aligned}
J(D) &= \left\| C(\cdot,\,\cdot,\,D) - C_i^{ob}(\cdot,\,\cdot) \right\|_\Omega^2 \\
&= \int\limits_0^T \int\limits_V \left(C(x,t,D) - C_i^{ob}(x,t) \right)^2 \mathrm{d}x\,\mathrm{d}t \to \min{}_p .
\end{aligned}
\tag{10}
$$

In (10), $C_i^{ob}(x,t)$ is the experimentally measured chemical dye concentration along the column obtained using the image processing technique, $C(x,t,D)$ is the calculated chemical dye concentration obtained from the analytical solution (7), $\Omega = V \times [0,T]$, $V = [0,l]$ and $(\cdot,\,\cdot,)$ refers to the independent variables. Usually the Output Least Squares identifiability is difficult to achieve due to observational errors; therefore, the OLS criterion (10) is usually regularized in the following manner (Tikhonov, 1963; Banks and Daniel, 1985):

$$
J(D) = \left\| C(\cdot,\,\cdot,\,D) - C_i^{ob}(\cdot,\,\cdot) \right\|_\Omega^2 + \beta \left\| D - D_0 \right\|_{U_D}^2 \to \min{}_p ,
\tag{11}
$$

where D_0 is an initial guess of the unknown parameter D and $\|\cdot\|_{U_D}$ is the norm in the observation space U_D. The second term in (11) is referred to as the *regularization term*, and $\beta > 0$ is defined as the regularization coefficient, which should be determined through the observation error (Miller, 1970; Kravaris and Seinfeld, 1985). In order to obtain a meaningful solution to the parameter identification problem, it is necessary to impose constraints on an admissible space K_{ad} of the parameter D. As further restrictions on the function space, we impose, respectively, the lower and upper limits D_l and D_u of D through the following constraint:

$$D_l \leqslant D \leqslant D_u. \tag{12}$$

The presence of these bounds ensures that the estimated parameters will be physically admissible.

It has been noted that due to its efficiency and accuracy, the Quasi-Newton Method (QNM) has been applied for the solution of the optimal problem in many areas in the engineering sciences (Engelman *et al.*, 1981; Soria and Pegon, 1990; Gottlieb and DuChateau, 1996). Yu (1998) provides a mathematical proof of the efficiency of the QNM in relation to parameter identification associated with parabolic partial differential equations. Therefore a Quasi-Newton iterative algorithm can be applied to solve either (10) or (11) subject to the constraint (12) to determine the hydrodynamic dispersion coefficient D consistent with the experimental data. In this algorithm the **BFGS** (Broyden–Fletcher–Goldfarb–Shanno) formula is used to determine the Jacobian matrix of the iteration consistent with the descent direction of the objective function $J(D)$ (Murray, 1972).

In general, it is difficult to calculate the descent orientation of $J(D)$ in a direct way, since the objective function in this optimization problem is complicated, and cannot be expressed as a straightforward mathematical function. Using the indirect method (Sun, 1994), however, it can be determined from the following:

$$-\nabla J(D) = -\iint\limits_{0\,V}^{T} \frac{\partial C}{\partial x} \frac{\partial \psi}{\partial x} \, dx \, dt, \tag{13}$$

where ψ is the *adjoint state* associated with the concentration C, which satisfies the following adjoint problem of the primary problem defined by (1)–(3), i.e.

$$\frac{\partial \psi}{\partial t} + \frac{\partial}{\partial x}(v\psi) + \frac{\partial}{\partial x}\left(D\frac{\partial \psi}{\partial x}\right) = 2(C - C^{ob}),$$

$$\psi(x, T) = 0; \quad D\frac{\partial \psi}{\partial x}\bigg|_{x=0,l} = 0, \quad x \in V, \quad t \in [0, T]. \tag{14}$$

4.2. PARAMETER IDENTIFICATION

For the purpose of the inverse analysis exercise, the results for the chemical dye distribution in the porous column derived from the experiment with constant advective velocity will be used for the identification of D. The seepage velocity during the transport process is determined from Darcy's law as $v_0 (= k(H_0 - H_D)/n^*l) = 2.18 \times 10^{-4}$ m/s. We note that the Reynolds number $\text{Re}(= v_0 d/v)$ associated with the flow is much smaller than unity; this confirms the applicability of Darcy's flow. With the analytical solution (7), the hydrodynamic dispersion coefficient D for the advective-dispersive transport of the chemical dye solution within the porous column is determined from the experimental results. The optimization procedure identified by (10) (or by (11) with $\beta = 0$) with constraint (12) is solved using the QNM, and the iterative results are listed in Table II with the initial value of D set at $D_0 = 5 \times 10^{-9}$ m²/s. Finally the hydrodynamic dispersion coefficient D is calculated as

$$D = 1.361 \times 10^{-8} \, \text{m}^2/\text{s}. \tag{15}$$

In general, the dispersion process associated with the movement of chemicals in porous media includes both *molecular diffusion* (D^*), which is governed by Fick's law, and *mechanical dispersion* (D_L), which is due to the velocity-induced mechanical mixing of the chemicals and pore fluids (Bear, 1972), i.e.

$$D = D_L + D^*. \tag{16}$$

Molecular diffusion is the primary process for controlling hydrodynamic diffusive processes in deposits with low advective velocity. Mechanical dispersion has a significant influence on contaminant transport in groundwater in porous media with relatively high hydraulic conductivity and advective hydraulic flow velocity within the limits applicable for Darcy flow. The coefficient of molecular diffusion D^* can be influenced by many factors in the transport processes in a porous medium and should be determined from results of experiments. The value of coefficient of molecular

Table II. Iterative evaluation of the hydrodynamic dispersion coefficient

D_0 (m²/s)	Iteration	J	$-\nabla J$	D (m²/s)	$\psi(n)$
5×10^{-9}	1	8.694×10^{-2}	4.686×10^2	1.147×10^{-8}	1.464×10^1
	2	2.317×10^{-2}	1.155×10^2	1.314×10^{-8}	4.626×10^1
	3	2.025×10^{-2}	7.230×10^1	1.361×10^{-8}	3.414×10^0

diffusion of the chemicals in a porous medium should, however, be less than that for the chemical species in water (i.e. $2.0 \times 10^{-9}\,\mathrm{m^2/s}$) (Freeze and Cherry, 1979). Based on the physical properties of glass beads and chemical components of the dye used in the experiment, the value of molecular diffusion in transport processes in the porous medium can be evaluated as $D^* = 1.0 \times 10^{-10}\,\mathrm{m^2/s}$ (Grathwohl, 1998). Therefore it is evident, from the values of D and D^*, that in the current series of experiments, the mechanical mixing is the dominant dispersive process during the transport process of chemical dye solution in the porous column.

The mechanical dispersion coefficient, D_L, is generally assumed to be a function of the magnitude of flow velocity (Taylor, 1953; Bear, 1972), and has the following form for one-dimensional problems

$$D_L = \alpha_L \, |v|, \tag{17}$$

where α_L is referred to as the longitudinal dispersivity and $|v|$ is a velocity norm. In multi-dimensional problems D_L will also depend on transverse dispersivity. With the determined values of D and D^* as well as Equations (16) and (17), the longitudinal dispersivity, α_L, of the chemical dye in the one-dimensional porous column can be evaluated as

$$\alpha_L = \frac{D - D^*}{|v|} = 6.186 \times 10^{-5}\,\mathrm{m}. \tag{18}$$

5. Computational Modelling of Advective-Dispersive Transport in the Column

5.1. STABILIZED SEMI-DISCRETE EULERIAN FINITE ELEMENT METHODS

There are two basic categories of numerical schemes that have been employed for solving advection-dispersion equations of the type described by (1). In the *fully discrete* approximation, the temporal and spatial terms in the equation are discretized together in the space–time domain $\Omega \times [0, T]$ and in the *semi-discrete* approximation, the equation is discretized spatially first via a numerical method (e.g. the finite difference method, the finite element method, or the boundary element method) and transformed into a first-order ordinary differential equation in time, which is solved using a time-integration scheme (e.g. Crank–Nicholson, Runge–Kutta methods, etc.). For advection-dominated transport problems (i.e. the elemental Péclet number $Pe = vh/D$ is much greater than unity), the conventional numerical schemes (e.g. Galerkin method) break down especially near sharp spatial gradient in the solution. This difficulty can be overcome by reducing the element size of the domain discretization, but this invariably leads to a

greater demand on computing resources. With the one-dimensional problem, this is not an issue, but with three-dimensional large-scale problems there will be additional demands on computing resources to achieve reliable and stable numerical results.

To date many stabilized *Semi-Discrete Eulerian* finite element methods have been developed for examining advection-dominated transport problems. The basic concept underlying these methods is to introduce artificial diffusion near the high gradient of the solution, by means of asymmetric weighting functions, to obtain the optimum computational performance. In the asymmetric weighting function thus referred to, a perturbation is introduced into the traditional Galerkin weighting function and this should be added to the "flow" direction to avoid crosswind diffusion (Hughes and Brooks, 1982). It therefore has the common factor $\alpha \mathbf{v} \cdot \nabla w$ (where α is called upwind function or intrinsic time of the stabilized methods (Oñate *et al.*, 1997); $\mathbf{v}$ is the characteristic velocity and w is a weighting function). The perturbation parameter, α, can be chosen based on either the Least Squares Methods, such that the artificial convection term has the adjoint form of a convection term in the equation and consequently the numerical scheme becomes symmetric (Wendland and Schmid, 2000), or be based on a Fourier analysis to ensure that numerical modelling can give an "optimal" solution for the transient advection-dispersion equation (Raymond and Garder, 1976), such as the Streamline Upwind Petrov–Galerkin Method (Hughes and Brooks, 1982). It can also take different values for the temporal term from the spatial term in the equation to generate different stabilized methods, such as the Taylor–Galerkin method.

The general residual integral equation, obtained in stabilized semi-discrete finite element methods, for the homogeneous advection-dispersion equation has the following form

$$\int_V \left[w + \alpha_1 \mathrm{sign}(v) \frac{\mathrm{d}w}{\mathrm{d}x} \right] \frac{C^{n+1} - C^n}{\Delta t} \, \mathrm{d}x + \int_V \left[w + \alpha_2 \, \mathrm{sign}(v) \frac{\mathrm{d}w}{\mathrm{d}x} \right] \times$$

$$\times \left(v \frac{\mathrm{d}C^{n+\theta}}{\mathrm{d}x} \right) \mathrm{d}x + \int_V D \frac{\mathrm{d}w}{\mathrm{d}x} \frac{\mathrm{d}C^{n+\theta}}{\mathrm{d}x} \, \mathrm{d}x = 0, \tag{19}$$

where $C^{n+\theta} = (1 - \theta)C^n + \theta C^n$ and θ is time-weighting. The expression for the upwind function, α_i $(i = 1, 2)$, for several stabilized finite element methods, the Petrov–Galerkin method (PG) (Hughes and Brooks, 1982), the second and third-order Taylor–Galerkin method (TG2 and TG3) (Donea *et al.*, 1984), the Least Squares method (LS) (Carey and Jiang, 1987) as well as the Modified Least Squares Method (MLS) (Wendland and Schmid, 2000; Selvadurai and Dong, 2005) are listed in the Table III, where h is the element length, Δt is the time step and the associated *Courant Number* is

$Cr = |v| \Delta t / h$. It can be seen from the residual integral Equation (19) that the perturbation in the asymmetric weighting function will introduce not only an "*artificial diffusion*" term but also an "*artificial convection*" term in the discretized form of the equation.

5.2. THE COMPARISON OF EXPERIMENTAL RESULTS AND COMPUTATIONAL ESTIMATES

In this section, the transport of a plug of chemical dye solution in the porous column is examined from experimental, analytical and computational perspectives. The experimental aspects have already been described in Section 3.1. The plug of chemical dye is 0.15 m in length and is located above the half way mark of the porous column of glass beads of length 0.61 m. The seepage velocity is spatially constant but decays exponentially with time, giving rise to flow velocities in the range $2.3 \times 10^{-4} \sim 2.0 \times 10^{-4}$ m/s during the progress of the experiment. The transport process can be described by the initial value problem given by (1) and (4), with $a = 0.15$ m and $b = 0.31$ m. The image processing method described in Section 3.2 is used to determine the transport process of the chemical dye plug via the colour distribution profile along the porous column. The experimental result for the normalized concentration derived from the image analysis and its variation with the dimensionless spatial and temporal variables $X = x/l$ and $T = kt/l$, respectively, is shown in Figure 9(a). The analytical result for the movement of the plug of dye solution determined by using the hydrodynamic dispersion coefficient obtained by combining the calculated value of hydrodynamic dispersivity α_L and the estimated coefficient of molecular diffusion D^* (described in Section 4.2) can be obtained from (5) by setting $a = 0.15$ m and $b = 0.31$ m. The results derived from this analytical solution are shown in Figure 9(b). Close resemblance of experimental results with the analytical solutions illustrates the effectiveness and accuracy of the image process technique for the determination of the concentration distribution of the dye during its migration through the porous column.

Table III. The upwind functions for the stabilized finite element schemes

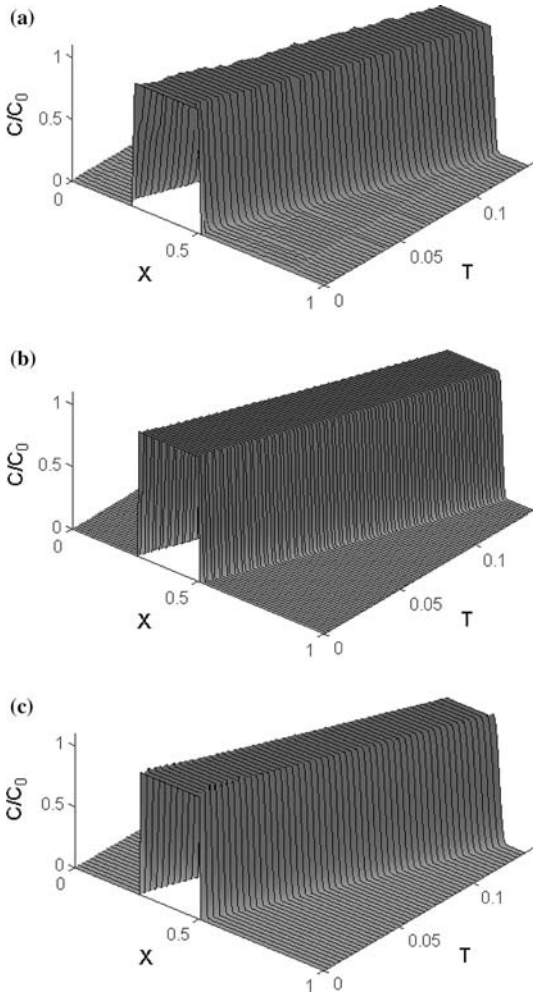| Methods	α_1	α_2
PG	$\frac{1}{\sqrt{15}} h$	$\frac{1}{\sqrt{15}} h$
TG2	0	$\frac{1}{2} |u| \Delta t$
TG3	$\frac{1}{6} |v|^2 \Delta t^2 \frac{\mathrm{d}}{\mathrm{d}x}$	$\frac{1}{2} |v| \Delta t$
LS	$\theta |v| \Delta t$	$\theta |v| \Delta t$
MLS	$\theta |u| \Delta t$	$\frac{4}{3} \theta |u| \Delta t$

Figure 9. A comparison of results for the time-dependent movement of a plug of chemical dye solution in a fluid-saturated porous column initiated by a time-dependent flow velocity, (a) experimental results, (b) analytical results, (c) numerical results obtained from the MLS method.

The transport of the plug of the dye solution can also be predicted via the computational modelling. Figure 9(c) shows the relevant numerical results for the initial value problem obtained from the MLS method using the transport parameters determined from separate experiments. In the numerical modelling, the Crank–Nicholson time integration scheme is used and the spatial domain is discretized into 200 elements with an elemental length of $h = 0.003$ m. Even with such a refined element size, the elemental Péclet number is greater than 48, which implies that for purposes
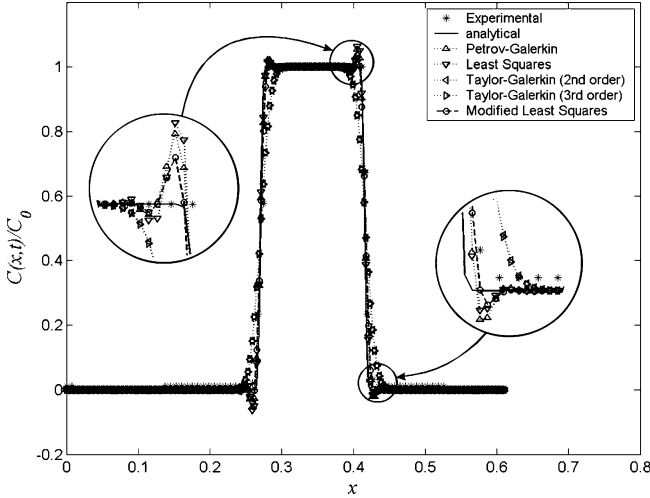
Figure 10. A comparison of experimental, analytical and numerical ($h = 0.003$ m) results for the transport of a plug of chemical dye in the porous column with decay in flow velocity ($t = 210$ s).

of the numerical modelling, the transport process of chemical dye solution in the porous column is largely advection-dominated. A Fourier analysis of the stabilized semi-discrete Eulerian finite element methods shows that these numerical methods will yield a better performance in terms of accuracy if the elemental Courant number is kept close to 0.5 (Selvadurai and Dong, 2005). Therefore, based on the magnitude of flow velocity, element length and the Courant number criterion $Cr \approx 0.5$, the time step is chosen as $\Delta t = 6$ s. In addition to the MLS scheme, four other stabilized semi-discrete Eulerian finite element methods (PG, LS, TG2 and TG3) are used to model the transport process concerning the movement of the plug of chemical dye solution in the porous column, using the same time increment and the time-marching scheme. Figure 10 shows the comparison of experimental results obtained from the image processing, the analytical solution given by (5) and computational estimates derived from the five stabilized schemes, evaluated at a specific time of $t = 210$ s. We note from results shown in Figure 10 that the different stabilized methods will have varied numerical performance for advection-dominated transport of the dye plug in the porous column. They either introduce the oscillations in the solution (e.g. PG, LS, and MLS) or are over-diffusive (TG2 and TG3) particularly near the steep gradient of the solution, and among these the MLS method can provide a reasonably good numerical estimate for the transport process particularly in the vicinity of the steep front.

Finally, the five stabilized methods are also used to examine the advective-dispersive transport of a dye solution in the porous column with
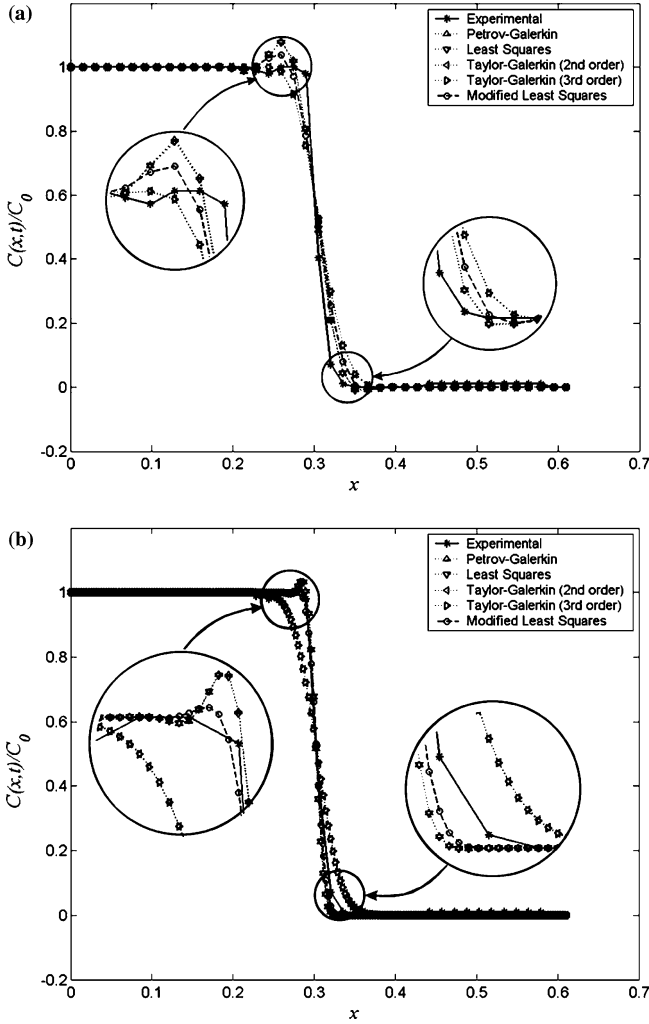
Figure 11. A comparison of experimental, analytical and numerical solutions at $t =$ 360 s for the transport of dye solution in a porous column with a time-dependent decaying flow velocity and different element length in the numerical modelling, (a) $h = 0.015$ m, (b) $h = 0.003$ m.

time-dependent velocities, in the range 6.8×10^{-4}–8.9×10^{-4} m/s. Two different mesh sizes $h = 0.015$ m and $h = 0.003$ m are considered in the numerical modelling, and the corresponding time steps are set to $\Delta t = 10$ s and $\Delta t = 2$ s, respectively, based on the elemental Courant number criterion $Cr \approx 0.5$. Figure 11 shows the comparison of the experimental results and the computational estimates, at $t = 360$ s, obtained from the five stabilized schemes where the computations are performed with coarse and fine mesh discretizations. The computational results shown in Figure 11 indicate

that mesh size has influence on the numerical performance of the stabilized methods and a relatively fine mesh is necessary, especially near the high gradient of the solution, to improve the computational accuracy.

6. Discussion and Concluding Remarks

A colour image processing technique is a useful tool for the quantitative determination of the distribution of the concentration of a chemical dye solution along observable locations of a porous column. The experimental results for the spatial distribution of the dye concentration are used to identify the hydrodynamic dispersion coefficient or longitudinal dispersivity associated with the transport processes. These parameters are used to test the applicability of an analytical solution to an initial value problem governing the transport of a chemical plug within a porous column, particularly under conditions of a time-dependent variation in the flow velocity. The close correlation between the results of the experiments and the analytical solution for the movement of a plug of chemical dye solution in the porous column, shown in Figures 9 and 10, indicates the effectiveness and accuracy of the image processing technique for estimating the distribution of dye concentration. The availability of experimental data and an analytical solution to the transport problem with variable flow velocity provides an opportunity to test the robustness of the stabilized computational schemes for the advection-dominated transport processes in terms of identifying the influences of numerically-induced diffusion. Five stabilized semi-discrete Eulerian finite element methods are considered for modelling the advection-dominated transport processes in the porous column with time-dependent flow velocity. A Crank–Nicholson time-integration scheme is used in the numerical scheme and the time step is chosen such that the elemental Courant number is close to 0.5 throughout the computations. The computational results for the advection-dominated transport process in the porous column with two different mesh sizes ($h = 0.015$ m and $h = 0.003$ m) support the observation that to obtain a better computational accuracy, a relative fine spatial discretization is needed for the stabilized methods especially in the vicinity of the sharp gradient of the solution. It should also be noted that despite the mesh refinement employed in the computations, certain numerical methods (such as TG2 and TG3) also produce an unwanted degree of numerical dispersion, and this numerical phenomenon can be examined by appeal to Fourier analysis.

A limitation of imaging techniques in their application to porous media is that the field of investigation is restricted to two-dimensional visualizations of the surface of the region of interest. Consequently, the transport phenomena obtained by a color image corresponds to the transport pattern of the chemical dye solution occurring between the wall of the glass tube

and the glass beads forming the porous medium. All analytical solutions, numerical estimates and inverse analysis apply to the transport process of the chemical dye solution on the cylindrical surface of the porous column. Since only one-dimensional transport processes are considered in this paper, a cylindrical glass container, rather than glass plane, is used in the experimental modelling. In order to minimize the optical distortions resulting from the curved surface of the glass tube, only images corresponding to a strip of narrow width are extracted from the image of the porous column of glass beads for the purposes of image processing. The ambient lighting conditions and colour of the solid particles and fluids being transported in the pore space are also important factors in the image processing approach. Calibration curves of the colour components of the truecolour image is a key part of the image processing exercise since it provides the mapping from the colour image to a digitized value of the dye concentration.

In this research, only advection-dominated transport processes of chemical dye solution are considered, the experimental results of which can be used to assess the capabilities of the stabilized computational schemes for simulating the advective transport of a steep front, which exhibits effects of numerical diffusion. The experimental facility is versatile to the extent that the diffusion-dominated transport process can also be examined by suitably altering the hydraulic conductivity characteristic of the porous medium and by maintaining sufficiently low hydraulic gradients and flow velocities to make the diffusive processes dominant. Also, with time-dependent boundary potential conditions, the transport problem involving the transition from an advection-dominated to a diffusion-dominated process can also be achieved.

In this paper, the advective-dispersive transport in a porous column with either a constant or time-dependent flow velocity fields is examined using experimental techniques, analytical methods and computational simulations. The investigation of the linearized transport problem is made complete by the identification of hydrodynamic dispersion coefficient via an inverse analysis. The results of the research should aid the experimentalist, the mathematical analyst and the numerical analyst to further advance each aspect of the problem.

Acknowledgement

References

Allersma, H. G. B.: 1982, Determination of the stress distribution in assemblies of photo-elastic particles, *Exp. Mech.* **9**, 336–341.

Allersma, H. G. B.: 1990, On line measurement of soil deformation in centrifuge tests by image processing, *9th Int. Conf. on Exp. Mech.* Copenhagen, 1739–1748.

Allersma, H. G. B.: 1998, Stress analysis on photoelastic particle assemblies in centrifuge tests, *Int. Conf. Centrifuge* **98**, Tokyo, 61–66.

Asundi, A. K.: 2002, *MATLAB for Photomechanics: A Primer*, Elsevier, Amsterdam, Boston, London.

Banks, H. T. and Daniel, P. L.: 1985, Estimation of variable coefficients in parabolic distributed system, *IEEE Trans. Auto. Control.* **AC-30**, 386–398.

Banks, R. B.: 1994, *Growth and Diffusion Phenomena: Mathematical Frameworks and Applications*, Springer-Verlag, Berlin.

Bear, J. and Bachmat, Y.: 1992, *Introduction to the Modelling of Transport Phenomena in Porous Media*, D. Reidel Publ. Co, Dordrecht, The Netherlands.

Bear, J.: 1972, *Dynamics of Fluids in Porous Media*, Dover Publications, New York.

Carey, G. F. and Jiang, B. N.: 1987, Least square finite element method and pre-conditioned conjugate gradient solution, *Int. J. Numer. Meth. Eng.* **24**, 1283–1296.

Caruana, A. and Dawe, R. A.: 1996, Experimental studies of the effects of heterogeneities on miscible and immiscible flow processes in porous media, *Transport in Chemical Eng.* **3**, 185–203.

Dagan, G.: 2004, Comment on "Exact averaging of stochastic equations for transport in random velocity field", *Transport Porous Media* **55**, 113–116.

Dawe, R. A., Wheat, M. R. and Biener, M. S.: 1992, Experimental investigation of capillary pressure effects on immiscible displacement in lensed and layered porous media, *Transport Porous Media* **7**, 83–101.

Donea, J., Giulian, S., Laval, H. and Quartapelle, L.: 1984, Time-accurate solution of advection-diffusion problem by finite elements, *Comput. Methods Appl. Mech. Eng.* **45**, 123–145.

Engelman, M. S., Strang, G. and Bathe, K. J.: 1981, The application of quasi-Newton methods in fluid mechanics, *Int. J. Numer. Meth. Engng.* **17**, 707–718.

Esposito, G., Allersma, H. G. B. and Selvadurai, A. P. S.: 1999, Geotechnical centrifuge modelling of LNAPL transport in partially saturated soil, *J. Geot. Geoenvironmental Eng.* **125**, 1066–1071.

Freeze, R. A. and Cherry, J. A.: 1979, *Groundwater*, Prentice-Hall, Englewood Cliffs, N.J.

Garboci, E. J., Bentz, D. P., and Martys, N. S.: 1999, Digital images and computer modeling, In *Experimental Methods in the Physical Sciences* **35**, *Method in the Physics of Porous Media*, Academic Press, San Diego, CA, Chapter 1, pp. 1–41.

Gelhar, L. W.: 1993, *Stochastic Subsurface Hydrology*, Prentice-Hall, Upper Saddle River, N.J.

Gonzalesz, R. C. and Woods, R. E.: 2002, *Digital Image Processing*, 2nd edn., Prentice Hall, Upper Saddle River, NJ.

Gottlieb, J. and Du Chateau, P. Eds.: 1996, *Parameter Identification and Inverse Problems in Hydrology, Geology, and Ecology*, Kluwer Academic Publishers, Dordrecht, Boston.

Grathwohl, P.: 1998, *Diffusion in Natural Porous Media: Contaminant Transport, Sorption/desorption and Dissolution kinetics*, Kluwer Academic Publishers, Boston.

Hughes, T. J. R. and Brooks, A.: 1982, A theoretical framework for Petrov-Galerkin methods with discontinuous weighting functions: Application to the Streamline-Upwind Procedure. in: R. H. Gallagher et al. (eds.), *Finite Elements in Fluids*, Vol. 4, Wiley, Chichester, pp. 47–65.

Kravaris, C. and Seinfeld, J. H.: 1985, Identification of parameters in distributed system by regularization, *SIAM J. Control Opt.* **23**, 217–241.

Lightfoot, N. M. H.: 1929, The solidification of molten steel, *Proc. London Math. Soc.* **31**, 97–116.

Lindstrom, F. T., Haque, R., Freed, V. H. and Boersma, L.: 1967, Theory on the movement of some herbicides in soils. Linear diffusion and convection of chemicals in soil, *Environ. Sci. Technol.* **1**, 561–565.

Macari, E. J., Parker J. K. and Costes N. C.: 1997, Measurement of volume changes in triaxial tests using digital imaging techniques, *Geotech. Testing J.* **20**, 103–109.

Miller, K. :1970, Least-squares methods for ill-posed problem with a prescribed bound, *SIAM J. Math. Anal.* **1**, 52–74.

Morton, K. W.: 1996, *Numerical Solution of the Convection-Diffusion Problem*, Chapman & Hall, London.

Murray, W. ed.: 1972, *Numerical Methods for Unconstrained Optimization*, Academic Press, London.

Ogata, A. and Banks, R. B.: 1961, A solution of the differential equation of longitudinal dispersion in porous media, *Geological Survey Professional Paper* 411-A, U.S. Govt. Printing Office, Washington, DC, A1–A7.

Oñate, E., García, J. and Idelsohn, S.: 1997, Computation of the stabilization parameter for the finite element solution of advective-diffusive problems, *Int. J. Numer. Meth. Fluids* **25**, 1385–1407.

Philips, O. M.: 1991, *Flow and Reactions in Permeable Rocks*, Cambridge University Press.

Rambidi, N. G. and Maximychev A. V.: 1994, Implementation of Image Processing Operations Using Light-Sensitive Chemical Dynamic Media, *Proceedings SPIE* **2430**, 90.

Rambidi, N. G., Maximychev, A. V. and Usatov, A. V.: 1995, Implementation of image processing operations using light-sensitive chemical dynamic media, *Opt. Memory Neural Networks* **4**, 99.

Raymond, W. H. and Garder, A.: 1976, Selective damping in a Galerkin method for solving wave problems with variable grids, *Monthly Weather Rev.* **104**, 1583–1590.

Selvadurai, A. P. S.: 2002, The advective transport of a chemical from a cavity in a porous medium, *Comput. Geotech.* **29**, 525–546.

Selvadurai, A. P. S.: 2003, Contaminant migration from an axisymmetric source in a porous medium, *Water Resour. Res.* **39**(6), 1204, WRR 001742.

Selvadurai, A. P. S.: 2004a, Advective transport from a penny-shaped crack in a porous medium and an associated uniqueness theorem, *Int. J. Numer. Analytical Meth. Geomech.* **28**, 191–208.

Selvadurai, A. P. S.: 2004b, On the advective-diffusive transport in porous media in the presence of time-dependent velocities, *Geophysical Res. Lett.* **31**, L13505, doi: 10.1029/2004GL019646.

Selvadurai, A. P. S. and Dong, W.: 2005, A Fourier analysis of semi-discrete Eulerian finite element methods for solution of the advection equation (In preparation).

Shvidler, M. and Karasaki, K.: 2003a, Exact averaging of stochastic equations for transport in a random velocity field, *Transport Porous Media* **50**, 223–241.

Shvidler, M. and Karasaki, K.: 2003b, Probability density functions for solute transport in random field, *Transport Porous Media* **50**, 243–266.

Soria, A. and Pegon, P.: 1990, Quasi-Newton iterative strategies applied to the heat diffusion equation, *Int. J. Numer. Meth. Eng.* **30**, 661–677.

Sun, N-Z: 1994, *Inverse Problems in Groundwater Modeling*, Kluwer Academic, Dordrecht; Boston.

Taylor, G. I.: 1953, Dispersion of soluble matter in solvent flowing slowly through a tube, *Proc. Roy. Soc. Ser. A*. **210**, 186–203.

Tikhonov, A. N.: 1963, Solution of ill-posed problems and the regularization method, *Soviet Math. Dokl.* **4**, 1035–1038.

Valliappan, S., Wang, W. and Khalili, N.: 1998, Contaminant transport under variable density flow in fractured porous media, *Int. J. Num. Anal. Meth. Geomech.* **22**, 575–595.

Vichnevetsky, R. and Bowles J. B.: 1982, *Fourier Analysis of Numerical Approximations of Hyperbolic Equations*, SIAM Philadelphia, P.A.

Wang, Y. and Hutter, K.: 2001, Comparisons of numerical methods with respect to convectively dominated problems, *Int. J. Numer. Meth. Fluids* **37**, 721–745.

Wendland, E. and Schmid, G. A.: 2000, Symmetrical Streamline Stabilization scheme for high advective transport, *Int. J. Numer. Anal. Meth. Geomech.* **24**, 29–45.

Yu, W.: 1998, A Quasi-Newton Approach to Identification of a Parabolic System, *J. Austral. Math. Soc. Ser. B* **40**, 1–22.

Zhao, C. B. and Valliappan, S.: 1994, Transient infinite elements for contaminant transport problems, *Int. J. Numer. Meth. Eng.* **37**, 1143–1158.